

## Design and Mechanism of Tetrahydrothiophene-based GABA Aminotransferase Inactivators

Hoang V. Le, Dustin D Hawker, Rui Wu, Emma H. Doud, Julia Reed Widom, Ruslan Sanishvili, Dali Liu, Neil L. Kelleher, and Richard B. Silverman

*J. Am. Chem. Soc.*, **Just Accepted Manuscript** • DOI: 10.1021/jacs.5b01155 • Publication Date (Web): 17 Mar 2015

Downloaded from <http://pubs.acs.org> on March 23, 2015

### Just Accepted

“Just Accepted” manuscripts have been peer-reviewed and accepted for publication. They are posted online prior to technical editing, formatting for publication and author proofing. The American Chemical Society provides “Just Accepted” as a free service to the research community to expedite the dissemination of scientific material as soon as possible after acceptance. “Just Accepted” manuscripts appear in full in PDF format accompanied by an HTML abstract. “Just Accepted” manuscripts have been fully peer reviewed, but should not be considered the official version of record. They are accessible to all readers and citable by the Digital Object Identifier (DOI®). “Just Accepted” is an optional service offered to authors. Therefore, the “Just Accepted” Web site may not include all articles that will be published in the journal. After a manuscript is technically edited and formatted, it will be removed from the “Just Accepted” Web site and published as an ASAP article. Note that technical editing may introduce minor changes to the manuscript text and/or graphics which could affect content, and all legal disclaimers and ethical guidelines that apply to the journal pertain. ACS cannot be held responsible for errors or consequences arising from the use of information contained in these “Just Accepted” manuscripts.



# Design and Mechanism of Tetrahydrothiophene-based GABA Aminotransferase Inactivators

Hoang V. Le,<sup>1</sup> Dustin D. Hawker,<sup>1</sup> Rui Wu,<sup>2</sup> Emma Doud,<sup>3</sup> Julia Widom,<sup>1</sup> Ruslan Sanishvili,<sup>4</sup> Dali Liu,<sup>2</sup> Neil L. Kelleher,<sup>3</sup> Richard B. Silverman<sup>\*,1</sup>

<sup>1</sup> Departments of Chemistry and Molecular Biosciences, Chemistry of Life Processes Institute, and the Center for Molecular Innovation and Drug Discovery, Northwestern University, Evanston, IL 60208

<sup>2</sup> Department of Chemistry and Biochemistry, Loyola University Chicago, Chicago, IL 60660

<sup>3</sup> Departments of Chemistry and Molecular Biosciences, and the Proteomics Center of Excellence, Northwestern University, Evanston, IL 60208

<sup>4</sup> X-ray Science Division, Advanced Photon Source, Argonne National Laboratory, Lemont, IL 60439

**ABSTRACT:** Low levels of  $\gamma$ -aminobutyric acid (GABA), one of two major neurotransmitters that regulate brain neuronal activity, are associated with many neurological disorders, such as epilepsy, Parkinson's disease, Alzheimer's disease, Huntington's disease, and cocaine addiction. One of the main methods to raise the GABA level in human brain is to use small molecules that cross the blood-brain barrier and inhibit the activity of  $\gamma$ -aminobutyric acid aminotransferase (GABA-AT), the enzyme that degrades GABA. We have designed a series of conformationally-restricted, tetrahydrothiophene-based GABA analogs with a properly-positioned leaving group that could facilitate a ring-opening mechanism, leading to inactivation of GABA-AT. One compound in the series is eight times more efficient an inactivator of GABA-AT than vigabatrin, the only FDA-approved inactivator of GABA-AT. Our mechanistic studies show that the compound inactivates GABA-AT by a new mechanism. The metabolite resulting from inactivation does not covalently bind to amino acid residues of GABA-AT but stays in the active site via H-bond interactions with Arg-192, a  $\pi$ - $\pi$  interaction with Phe-189, and a weak nonbonded S...O=C interaction with Glu-270, thereby inactivating the enzyme.

## 1. Introduction

Epilepsy is a family of chronic neurological disorders characterized by recurring convulsive seizures, which result from abnormal, excessive neuronal activity in the central nervous system.<sup>1</sup> It is estimated that about 65 million people worldwide have epilepsy.<sup>2</sup> Epilepsy can arise from an imbalance in two major neurotransmitters that regulate brain neuronal activity, *L*-glutamate, an excitatory neurotransmitter, and  $\gamma$ -aminobutyric acid (GABA), an inhibitory neurotransmitter.<sup>3</sup>

GABA is produced in GABAergic neurons from *L*-glutamate by the enzyme glutamic acid decarboxylase (GAD) (Figure 1).<sup>4,5</sup> GABA is then released into the synapse and transported to glial cells. The enzyme GABA aminotransferase (GABA-AT) in glial cells degrades GABA to succinic semialdehyde, which is further oxidized to succinate and enters the Krebs cycle. In this first half of the GABA-AT catalytic cycle, cofactor pyridoxal 5'-phosphate (PLP) is converted to pyridoxamine 5'-phosphate (PMP). GABA-AT also converts  $\alpha$ -ketoglutarate from the Krebs cycle to *L*-glutamate and returns PMP to PLP in the second half of its catalytic cycle. Because there is no GAD in glial cells, this newly formed *L*-glutamate is not converted to GABA. It is instead converted to *L*-glutamine, which is then released

from glial cells into the synapse and transported back to GABAergic neurons to complete the metabolic cycle of *L*-glutamate.

Low levels of GABA are linked to not only epilepsy,<sup>6</sup> but also many other neurological disorders including Parkinson's disease,<sup>7</sup> Alzheimer's disease,<sup>8</sup> Huntington's disease,<sup>9</sup> and cocaine addiction.<sup>10</sup> Raising GABA levels has proven effective in stopping recurring convulsive seizures in the treatment of epilepsy.<sup>11</sup> However, GABA does not cross the blood-brain barrier; therefore, an increase in brain levels of GABA cannot be achieved by intravenous administration.<sup>12</sup> To increase brain levels of GABA, one could speed up the activity of GAD, the enzyme that makes GABA, inhibit the activity of GABA-AT, the enzyme that degrades GABA, or inhibit the reuptake of GABA by blocking the action of the GABA transporters.

Our laboratory has focused on the design of mechanism-based inactivators of GABA-AT, unreactive compounds that require GABA-AT catalysis to convert them into the species that inactivates the enzyme. Because these molecules are not initially reactive, but require the catalytic activity of GABA-AT to become activated and form covalent bonds, indiscriminate reactions with off-target proteins, leading to undesired side effects, should be greatly reduced. Even at lower dosages, these inactivators can

achieve the desired pharmacologic effects with enhanced potency and selectivity than conventional inhibitors.<sup>13</sup>

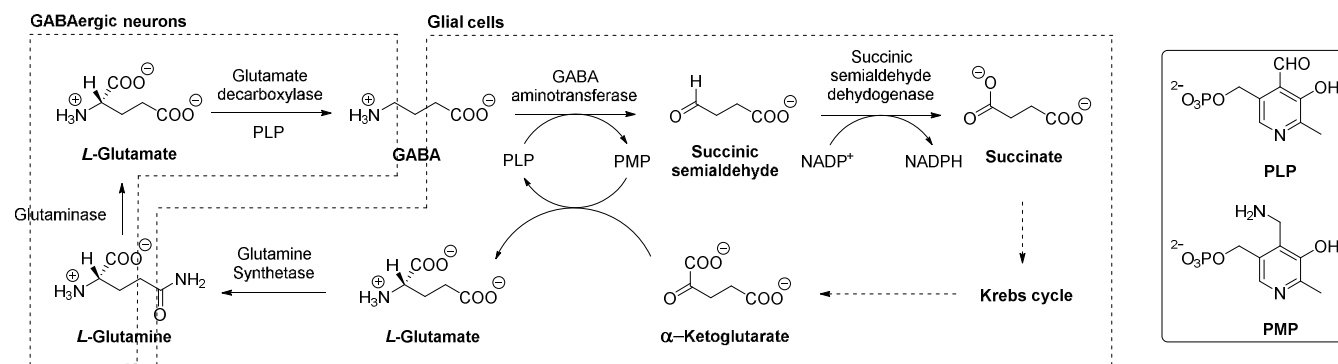
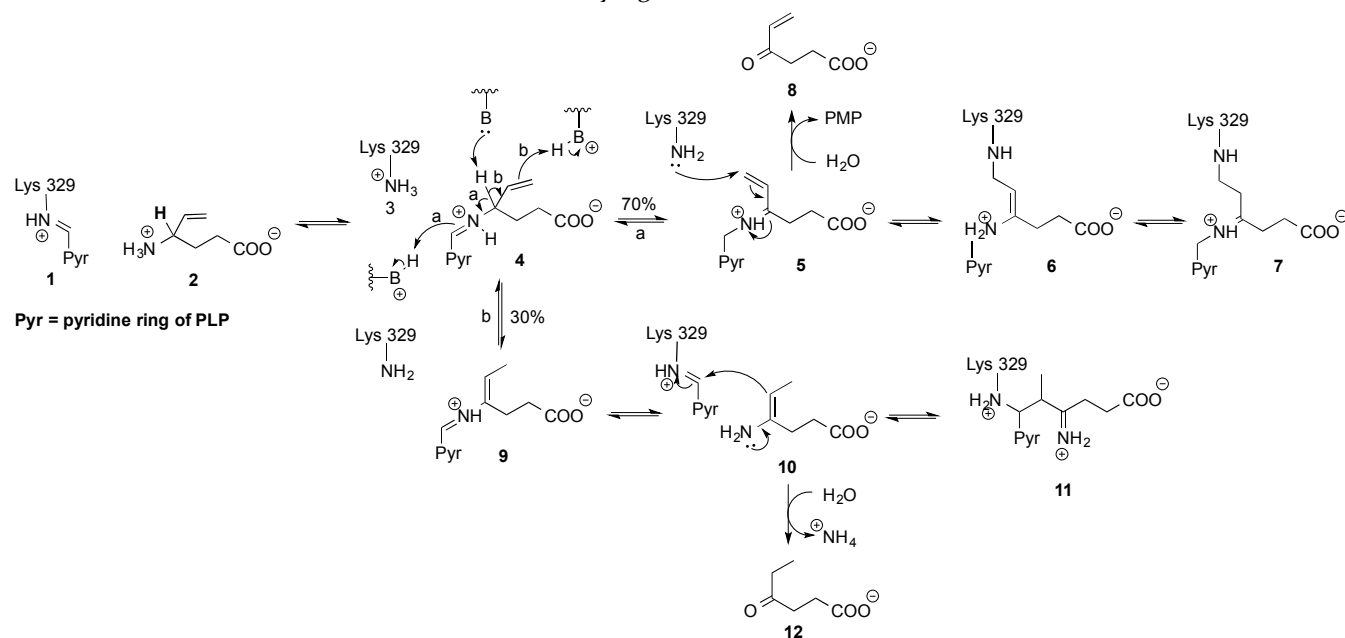


**Figure 1.** Metabolic cycle of *L*-glutamate

**Scheme 1.** Mechanisms of inactivation of GABA-AT by vigabatrin



Currently, the only FDA-approved inactivator of GABA-AT is the drug vigabatrin (**2**) (Scheme 1), which was first developed by Lippert *et al.*,<sup>14</sup> and is used for the treatment of epilepsy.<sup>15</sup> However, a large dose of vigabatrin (1 – 3 g) needs to be taken daily,<sup>16–18</sup> and there are many serious side effects that arise from its usage, including psychosis<sup>19</sup> and permanent vision loss resulting from the damage of the retinal nerve fiber layer.<sup>20</sup> Therefore, the demand for an alternative to vigabatrin in the treatment of epilepsy is urgent.

We have found that vigabatrin inactivates GABA-AT via two pathways: a Michael addition mechanism and an enamine mechanism, as shown in Scheme 1.<sup>21</sup> In the Michael addition mechanism, the resulting Schiff base (**4**) from the reaction of vigabatrin and the lysine-bound PLP (**1**) on GABA-AT is subjected to  $\gamma$ -proton (boldfaced hydrogen in **2**) removal and tautomerization that leads to

ketimine **5**. An active-site nucleophile then reacts with Michael acceptor **5** to form **6**, which is in equilibrium with **7**. In the enamine mechanism, the Schiff base (**4**) is subjected to  $\gamma$ -proton removal and tautomerization through the vinyl bond, which leads to the release of enamine **10**. Subsequent nucleophilic addition of **10** to the lysine-bound PLP on GABA-AT gives rise to **11**.

The Michael addition mechanism and the enamine mechanism happen concurrently in a 70/30 ratio, respectively. It was discovered that ketimine **5** in the Michael addition mechanism, and enamine **10** in the enamine mechanism, underwent partial hydrolysis to form the  $\alpha,\beta$ -unsaturated ketone (**8**) and the saturated ketone (**12**), respectively. While **8** is a reactive electrophile, possibly responsible for some side effects, **12** is not a reactive metabolite. Therefore, it is imperative to find vigabatrin analogs that either follow the enamine mechanism exclusively to avoid the

formation of **8** or speed up the Michael addition pathway so that **5** would have much lower probability to undergo hydrolysis.

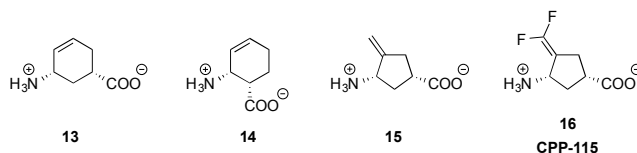
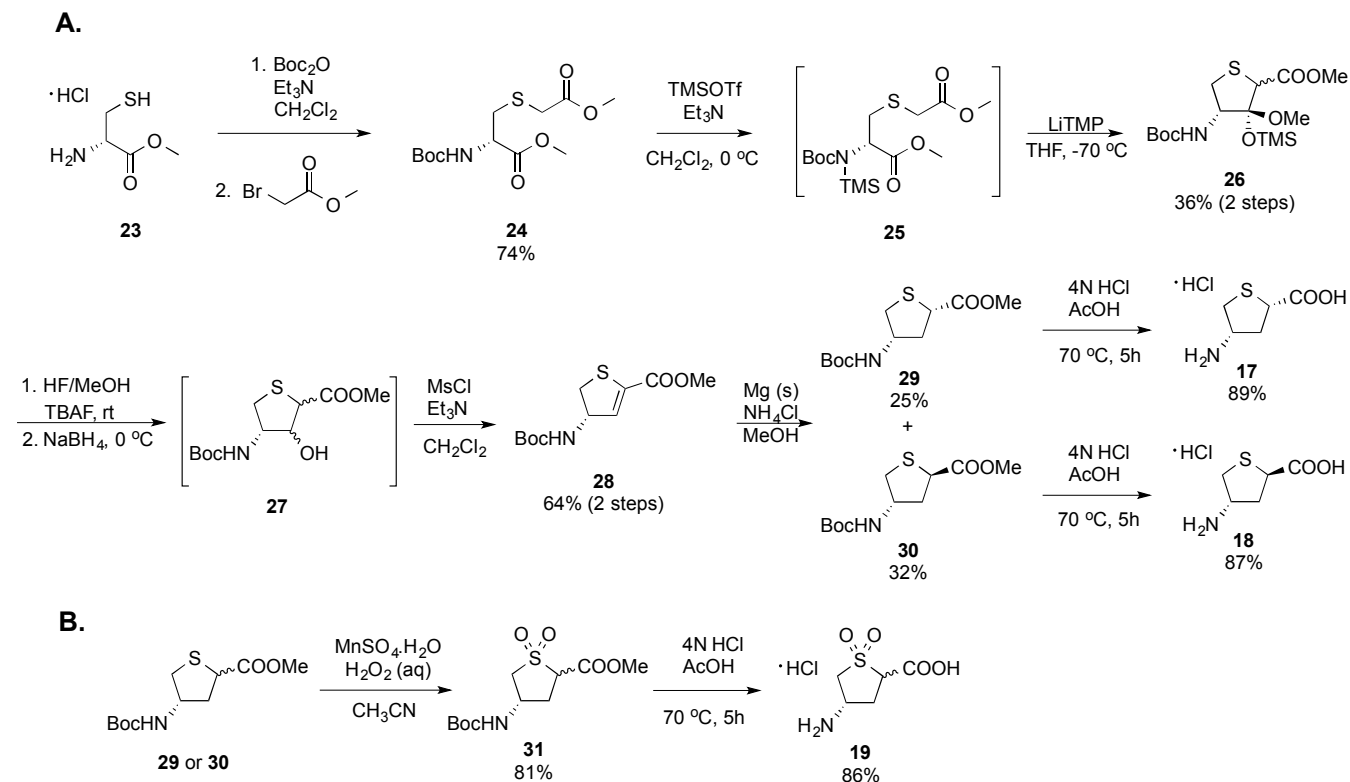


**Figure 2.** Vigabatrin analogs that follow one GABA-AT inactivation mechanism exclusively

**Scheme 3.** Syntheses of GABA Analogs **17** – **19**



An energy minimized molecular model of vigabatrin bound to PLP in GABA-AT revealed that after tautomerization, the vinyl bond in **5** needs to rotate toward Lys-329 for the Michael addition to occur.<sup>22</sup> Therefore, conformationally-restricted analogs such as **13** and **14** (Figure 2) would prevent the rotation of the vinyl bond, thereby blocking the Michael addition mechanism. Experiments showed that **13** inactivated GABA-AT following the enamine mechanism exclusively. However, its potency remained low. In the alternative approach, conformationally-restricted analogs **15** and **16** have the vinyl bond readily pointed toward Lys-329 for rapid Michael addition to occur, thereby minimizing the hydrolysis of the ketimine intermediate.<sup>23</sup> Experiments showed that **16** was 186 times more efficient in inactivating GABA-AT than vigabatrin. Furthermore, unlike vigabatrin,<sup>24</sup> **16** did not inactivate or inhibit off-target enzymes, such as alanine aminotransferase and aspartate aminotransferase,<sup>25</sup> and therefore is less likely to produce side effects. Indeed, we tested **16** in a multiple-hit rat model of infantile spasms,<sup>26</sup> and the results showed that **16** suppressed spasms at doses of 0.1-1 mg/kg/day, which were >100-fold lower than those for vigabatrin. The spasms suppression by **16** stayed effective longer (3 days vs. 1 day for vigabatrin), and **16**

also had a much larger margin of safety than vigabatrin. With those results, **16**, now known as CPP-115, was granted Orphan Drug Designation by the FDA for the treatment of infantile spasms. It recently finished a Phase I clinical trial.

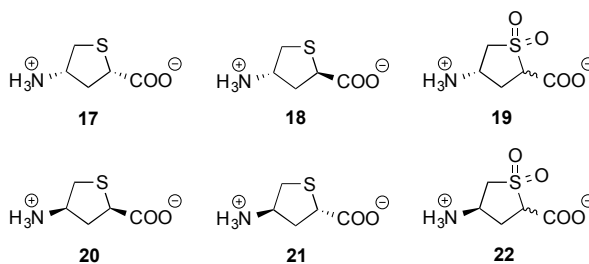
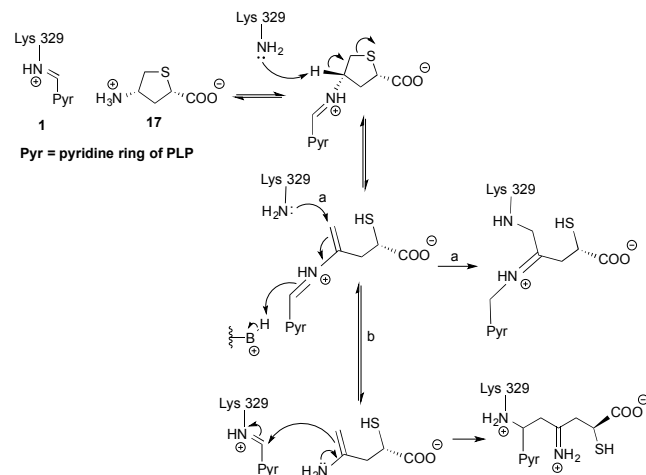


**Figure 3.** Tetrahydrothiophene-based GABA analogs

In our ongoing effort to develop new classes of antiepileptic drugs, we are interested in new GABA analogs that inactivate GABA-AT by new mechanisms. Compounds with a leaving group adjacent to the carbanion formed after the  $\gamma$ -proton removal seem to inactivate GABA-AT by an enamine mechanism. Therefore, we synthesized a series of conformationally-restricted, tetrahydrothio-

phene-based analogs (Figure 3), which have a properly-positioned leaving group that could facilitate a ring-opening mechanism in the inactivation of GABA-AT (Scheme 2). Here we report the synthesis, biological evaluation, mechanistic studies, including mass spectral and X-ray crystallographic results, of these analogs, which reveal an unexpected inactivation mechanism.

**Scheme 2.** Michael addition (pathway a) and enamine addition (pathway b) mechanisms for **17**



## 2. Results and Discussion

The syntheses of analogs **17** – **19** are shown in Scheme 3, starting from commercially available *D*-cysteine methyl ester hydrochloride (**23**). The route up to the generation of dihydrothiophene **28** was achieved by following a modified procedure from Adam *et al.*<sup>27</sup> Reduction of **28** by magnesium in methanol resulted in diastereomers **29** and **30**, which were separable by flash column chromatography. Deprotection of the amino group and hydrolysis of the ester in **29** and **30** using aqueous HCl provided the desired analogs **17** and **18**, respectively. Oxidation of **29** or **30** by  $\text{MnSO}_4$  and  $\text{H}_2\text{O}_2$  resulted in a 1:1 mixture of the corresponding sulfones (**31**) as a result of epimerization at the C-2 position. Subsequent deprotection of the amino group and hydrolysis of the ester in **31** using aqueous HCl gave desired analog **19**. Synthesis of compounds **20** – **22** followed an identical route starting from *L*-cysteine methyl ester hydrochloride. The purity of compounds **17** – **22** was confirmed by HPLC and HRMS, which showed that there was none of the corresponding dihydrothiophene analog of **17**, a known inactivator of GABA-AT.<sup>28</sup>

Preliminary *in vitro* results showed that **19** – **22** were weak reversible inhibitors, while **17** and **18** were potent inactivators of GABA-AT (Table 1). The kinetic constants for inactivation of GABA-AT by **17** and **18** could not be determined accurately under optimal conditions (pH 8.5, 25 °C),<sup>23</sup> where the enzyme exhibited maximum activity, because inactivation occurred too rapidly. The inhibition constant ( $K_i$ ) and the rate constant of enzyme inactivation ( $k_{\text{inact}}$ ) for inactivation of GABA-AT by **17** and **18** were then measured under non-optimal conditions (pH 6.5, 25 °C) using a Kitz and Wilson replot.<sup>29</sup> From  $k_{\text{inact}}/K_i$  values (Table 1), we can conclude that **17** is eight times more efficient an inactivator of GABA-AT than vigabatrin (with an

inactivation rate constant almost 20 times that of vigabatrin), and **18** is half as efficient as vigabatrin.

**Table 1.** Kinetic constants for the inhibition and inactivation of GABA-AT by **17** – **19**

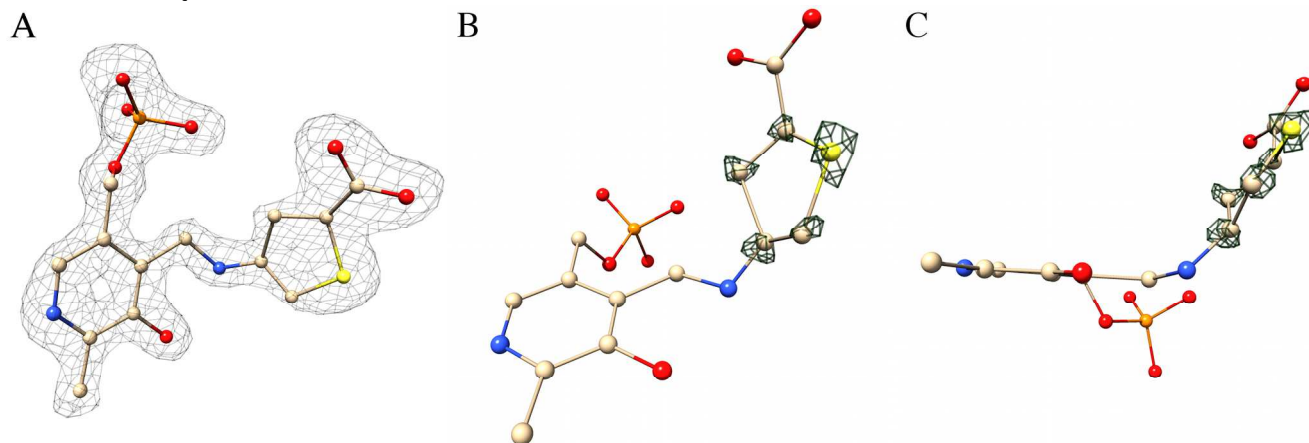
Compound	$K_i$ (mM)	$k_{\text{inact}}$ ( $\text{min}^{-1}$ )	$k_{\text{inact}}/K_i$ ( $\text{min}^{-1} \text{mM}^{-1}$ )	$K_i$ (mM)
<b>17</b>	0.182	0.17	0.93	-
<b>18</b>	2.23	0.12	0.05	-
<b>19</b>	-	-	-	$3.2 \pm 0.7$
<b>20</b>	-	-	-	$3.4 \pm 0.8$
<b>21</b>	-	-	-	$3.3 \pm 0.7$
<b>22</b>	-	-	-	$7.5 \pm 0.7$
(S)-vigabatrin	3.2	0.37	0.11	-

The X-ray crystal structure GABA-AT inactivated by **17** (at 1.66 Å) showed that the inactivating metabolite contained a buckled 5-membered ring covalently bound to PLP (Figure 4A), and Lys-329 was not covalently modified. The final ligand interpretation is strongly supported by the electron density of the simulated annealing omit map (fo-*fc*). Furthermore, the omit map density at a higher contour level also revealed that the refined atom positions of the dihydrothiophene ring were accurate, resulting in a nonplanar ring (Figures 4B, 4C). (*S*)-4-Amino-4,5-dihydro-2-thiophenecarboxylic acid, the corresponding dihydrothiophene analog of **17**, is a known inactivator of GABA-AT that inactivates by an aromatization mechanism resulting in a thiophene ring;<sup>28</sup> it also is an inactivator of aspartate aminotransferase.<sup>30</sup> Here, the crystal structure of **17**-inactivated GABA-AT suggests that the inactivation by **17** is likely to follow the mechanism shown in Scheme 4. The resulting Schiff base (**32**) from the reaction of **17** and the lysine-bound PLP on GABA-AT undergoes  $\gamma$ -proton removal, leading to enamine **34**. The crystal structure revealed that **34** was stabilized in the active site by an interaction between its carboxylate group and the guanidinium group of Arg-192, by the interaction between the enamine alkene and the phenyl ring of Phe-189, and the sulfur atom in **34** is in close proximity (3.3 Å) to a carboxyl oxygen atom of Glu-270 (Figure 5A). This distance suggests a weak nonbonded interaction between the divalent sulfur and the carboxyl carbonyl oxygen. Weak nonbonded S...O and S...N interactions have been reported and are mainly characterized as stabilizing forces of protein structures<sup>31</sup> and of some organic sulfur compounds.<sup>32,33</sup> These interactions have recently attracted growing attention because they could play important roles in the structure and the biological activity of some sulfur compounds and might also regulate enzymatic functions.<sup>34</sup> Until now, all reported weak nonbonded interactions have been intramolecular. To the best of our knowledge, no intermolecular weak nonbonded S...O and S...N interactions have been reported. However, the distance and directionality of intermolecular nonbonded S...O interactions has been suggested in theoretical studies.<sup>34</sup> For intermolecular nonbonded S...O interactions, the nucleophilic O atom approaches the S atom from the backside of the S - Y and S - Z bonds (the  $\sigma_s^*$  direction), and the S atom lies in the direction of the O lone pairs (the  $n_O$  direction) (Figure 5B). The stabilization of this

1  
2  
3  
4  
5  
6  
7  
8  
9  
10  
11  
12  
13  
14  
15  
16  
17  
18  
19  
20  
21  
22  
23  
24  
25  
26  
27  
28  
29  
30  
31  
32  
33  
34  
35  
36  
37  
38  
39  
40  
41  
42  
43  
44  
45  
46  
47  
48  
49  
50  
51  
52  
53  
54  
55  
56  
57  
58  
59  
60

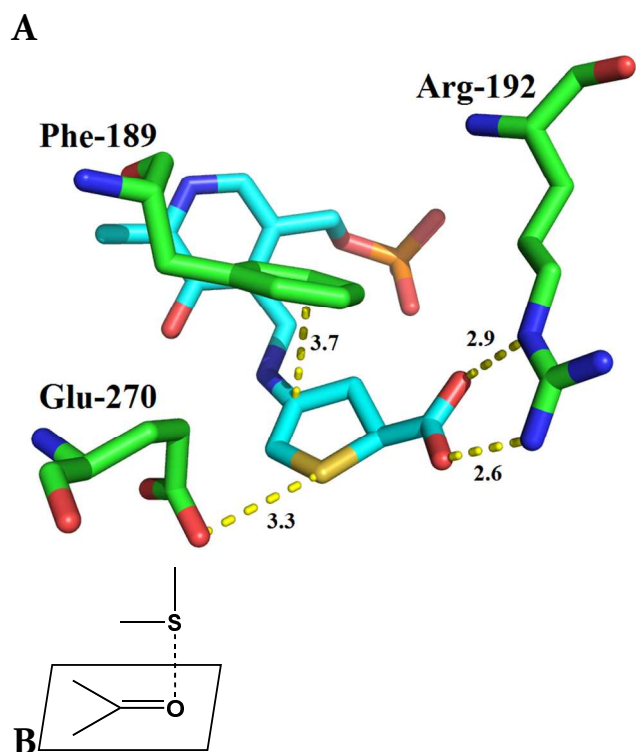
S...O=C interaction is described by an  $n_{\text{O}} \rightarrow \sigma_{\text{C}}^*$  orbital interaction, and 3.3 Å is well within the predicted distance. As shown in Figure 5A, the directionality of the interaction between the sulfur atom in metabolite **34** and the carboxyl group of Glu-270 matches the description of the directionality of theoretical intermolecular nonbond-

ed S...O interactions. Therefore, the interaction between the sulfur atom in metabolite **34** and the carboxyl group of Glu-270 might be the first reported example of an intermolecular nonbonded S...O interaction, which contributes to the stabilization of metabolite **34** in the active site of GABA-AT.



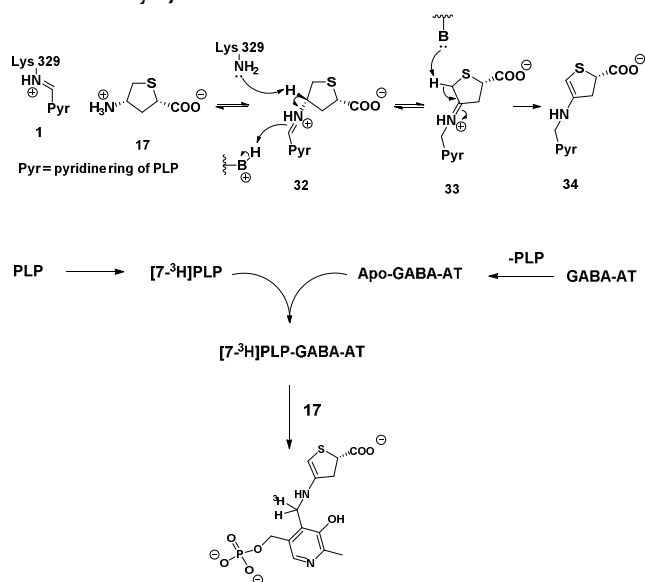
**Figure 4.** The PLP-dihydrothiophene complex, shown in ball-and-stick form, is the final adduct, which contains a non-planar dihydrothiophene ring. Carbons are in beige, nitrogens are in blue, oxygens are in red, phosphorus is in orange, and sulfur is in yellow. (A) The electron density of the simulated annealing omit map ( $f_o - f_c$ ) is shown as a grey mesh at 3.5  $\sigma$  around the PLP-dihydrothiophene adduct. (B) and (C) are two different orientations of the same image: the electron density of the simulated omit map ( $f_o - f_c$ ) is shown in green mesh at 4.1  $\sigma$  around atoms in the dihydrothiophene ring (at a 0.6 Å radius). (B) This orientation displays the refined atom positions; (C) this orientation displays a buckled ring plane.

tionality of the intermolecular weak nonbonded S...O interaction in theoretical studies,<sup>34</sup> representing an  $n_{\text{O}} \rightarrow \sigma_{\text{C}}^*$  orbital interaction



**Figure 5.** (A) Interactions between the PLP-dihydrothiophene adduct and nearby residues. (B) Direc-

**Scheme 4.** Proposed mechanism for the inactivation of GABA-AT by **17**



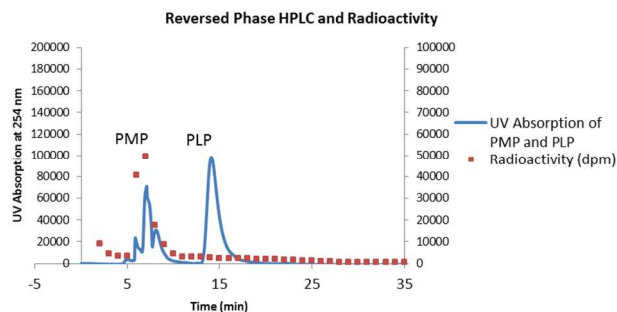
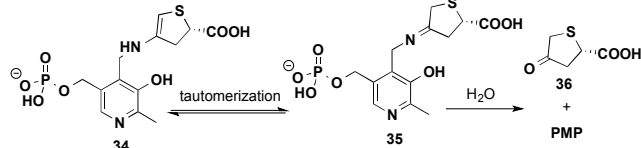


**Figure 6.** Radioactive-labeling experiment for the inactivation of GABA-AT by **17**: [ $7\text{-}^3\text{H}$ ]PLP-GABA-AT was prepared from apoGABA-AT and [ $7\text{-}^3\text{H}$ ]PLP then inactivated by **17**, followed by denaturation and submission to HPLC. Fractions were collected each minute and counted for radioactivity. A solution of 1 mM PMP and 1 mM PLP was treated identically as a control.

Mass spectrometric analysis (via ESI-mass spectrometry) was run on a sample of GABA-AT, inactivated by **17**, but the presence of **34** was not observed. When a small amount of formic acid was added to another sample of GABA-AT inactivated by **17** to disrupt H-bonding before running the spectrum, metabolite **36** ( $m/z$  144.9954, Supporting Information Figure S1) was detected instead of **34**. Fragmentation data for  $m/z$  144.9954 confirmed the structure of **36** (Supporting Information Figure S2), the likely result of hydrolysis of **34** (Scheme 5).

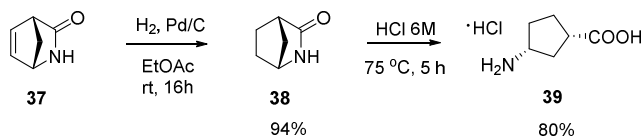
#### Scheme 5. Hydrolysis of Metabolite **34**



Treatment of [ $7\text{-}^3\text{H}$ ]PLP-reconstituted GABA-AT with **17** was performed to determine the fate of the coenzyme upon inactivation. A solution of 1 mM PMP and 1 mM PLP was treated identically as controls. The results showed that the denaturation of GABA-AT, inactivated by **17**, released PMP exclusively (Figure 6).

Results from the radioactive-labeling experiment and mass spectrometric analysis suggested that metabolite **34** was not stable outside of the active site and would undergo hydrolysis to produce PMP and **36**, supporting the proposed mechanism for the inactivation of GABA-AT by **17** shown in Scheme 4.

#### Scheme 6. Synthesis of Cyclopentane Analog **39**



If the interaction between the sulfur atom in **34** and the O=C of Glu-270 is an intermolecular nonbonded S...O interaction, then the corresponding cyclopentane analog (**39**) (Scheme 6) should form a less stable metabolite in the active site of GABA-AT than **34**. We have made and

investigated the activity of **39** from (1*S*,4*R*)-2-azabicyclo[2.2.1]hept-5-en-3-one (**37**, Scheme 6). Results showed that **39** is not an inactivator but is a good competitive inhibitor of GABA-AT with a  $K_i$  of 0.87 mM. A computer model of the energy-minimized hypothetical adduct of **39** bound to PLP after tautomerization and deprotonation (i.e., the cyclopentene analog of **34**) docked into GABA-AT using GOLD<sup>35</sup> gave the pose with the highest fitness score that was almost identical to that shown in Figure 5 (Supporting Information Figure S25). These inhibition and modeling results further support the crucial role of the sulfur atom in retaining the product in the active site of GABA-AT, thereby inactivating the enzyme.

### 3. Conclusion

We have developed two new GABA-AT inactivators. Preliminary *in vitro* results show that **17** is eight times more efficient an inactivator of GABA-AT than vigabatrin, an FDA-approved antiepilepsy drug, and **18** is half as efficient as vigabatrin. Mechanistic studies of the inactivation of GABA-AT by **17** showed that the sulfur atom in **17** plays a crucial role in keeping the resulting adduct bound to the active site of GABA-AT, thereby inactivating the enzyme. An intermolecular nonbonded interaction between the carboxyl oxygen of Glu-270 and the sulfur atom in **17**, the first observed example of this kind, is important for stabilizing the adduct in the active site.

### 4. Experimental Section

#### General Procedures

Chemicals were obtained from TCI America, Sigma-Aldrich, Alfa Aesar, and American Radiolabeled Chemicals, and used as received unless specified. All syntheses were conducted under anhydrous conditions in an atmosphere of argon, using flame-dried apparatus and employing standard techniques in handling air-sensitive materials, unless otherwise noted. All solvents were distilled and stored under an argon or nitrogen atmosphere before use.  $^1\text{H}$  NMR and  $^{13}\text{C}$  NMR spectra were taken on a Bruker AVANCE III 500 spectrometer using  $\text{CDCl}_3$ , MeOD,  $(\text{CD}_3)_2\text{CO}$ , or  $\text{D}_2\text{O}$  as solvents, recorded in  $\delta$  (ppm) and referenced to  $\text{CDCl}_3$  (7.26 ppm for  $^1\text{H}$  NMR and 77.16 ppm for  $^{13}\text{C}$  NMR) or MeOD (3.31 ppm for  $^1\text{H}$  NMR and 49.00 ppm for  $^{13}\text{C}$  NMR) or  $(\text{CD}_3)_2\text{CO}$  (2.05 ppm for  $^1\text{H}$  NMR and 29.84 ppm for  $^{13}\text{C}$  NMR) or  $\text{D}_2\text{O}$  (4.79 ppm for  $^1\text{H}$  NMR). Nuclear Overhauser Effect (NOE) correlation experiments were performed using an Agilent DDR2 400 MHz spectrometer. High resolution mass spectra (HRMS) were measured with an Agilent 6210 LC-TOF (ESI, APCI, APPI) mass spectrometer. The purity of the synthesized final compounds was determined by HPLC analysis to be >95%. The column used was a Chiralcel OD-H 5  $\mu\text{m}$ , 4.6 x 250 mm. After thorough column equilibration, compounds were eluted with a mobile phase of 2% EtOH in hexanes at 0.6 mL/min. Biochemical assays were performed using a Biotek Synergy H1 microplate reader. Prior to their evaluation, initial experiments were performed to confirm the synthesized analogues do not inhibit the

coupling enzymes utilized in the substrate and inhibition assays. Mass spectrometric analysis: LC gradient was employed at a flow rate of 200  $\mu\text{L}/\text{min}$  on an Agilent 1150 LC system (Agilent, Santa Clara, CA, USA); mass spectrometry was performed on a Q-Exactive mass spectrometer (Thermo Fisher Scientific, Waltham, MA, USA). Crystallographic data were collected on beamlines 23ID-B and 23ID-D of GM/CA@APS of the Advanced Photon Source (APS) using X-rays of 0.99  $\text{\AA}$  wavelength and Rayonix (formerly MAR-USA) 4x4 tiled CCD detector with a 300  $\text{mm}^2$  sensitive area.

**(S)-Methyl 2-((tert-butoxycarbonyl)amino)-3-((2-methoxy-2-oxoethyl)thio)propanoate (24)**

To a stirred light suspension of *D*-cysteine methyl ester hydrochloride (**23**, 5 g, 29.1 mmol) and  $\text{Boc}_2\text{O}$  (7 mL, 30.6 mmol) in anhydrous  $\text{CH}_2\text{Cl}_2$  (250 mL) at 0  $^\circ\text{C}$  was added  $\text{Et}_3\text{N}$  (15.4 mL, 111 mmol) over a 10 min period. After addition, the cooling bath was removed, and the reaction solution was stirred at rt overnight. After being cooled to 0  $^\circ\text{C}$ , methyl bromoacetate (3.3 mL, 35 mmol) was added to the reaction solution and was stirred for 30 min before removal of the cooling bath. Stirring was continued for 2 h at rt, followed by removal of the bulk of the solvent under reduced pressure. The resulting crude mixture was diluted with ether (60 mL), washed with water (3 x 30 mL) and brine (5 mL), dried ( $\text{MgSO}_4$ ), and concentrated. Chromatography (ethyl acetate/hexanes, 3:7) afforded the desired product as a clear oil (6.79 g, 74%).  $^1\text{H}$  NMR matched literature value.<sup>27</sup>  $^1\text{H}$  NMR (500 MHz,  $\text{CDCl}_3$ )  $\delta$  5.40 (d,  $J$  = 8.2 Hz, 1H), 4.55 (m, 1H), 3.75 (s, 3H), 3.73 (s, 3H), 3.26 (q,  $J$  = 15.2 Hz, 2H), 3.07 (m, 2H), 1.43 (s, 9H).  $^{13}\text{C}$  NMR (126 MHz,  $\text{CDCl}_3$ )  $\delta$  171.50, 170.61, 155.27, 80.35, 53.16, 52.78, 52.66, 35.02, 33.90, 28.38. HRMS (LC-TOF): Calculated for  $\text{C}_{12}\text{H}_{21}\text{NO}_6\text{S}$  [ $\text{M}+\text{Na}$ ]<sup>+</sup> 330.0982; found 330.1001.

**(3R,4S)-Methyl 4-((tert-butoxycarbonyl)amino)-3-methoxy-3-((trimethylsilyloxy)tetrahydrothiophene-2-carboxylate (26)**

To a solution of **24** (6.59 g, 21.4 mmol) in anhydrous dichloromethane (100 mL) at 0  $^\circ\text{C}$  was added  $\text{Et}_3\text{N}$  (3.3 mL, 23.6 mmol) followed by dropwise addition of TMSOTf (4.25 mL, 23.5 mmol) over 20 min. The mixture was stirred for 10 min at 0  $^\circ\text{C}$  then allowed to warm to rt. After being quenched with saturated sodium bicarbonate (50 mL), the organic layer was separated and washed with saturated  $\text{NaHCO}_3$  (2 x 50 mL), dried ( $\text{MgSO}_4$ ) and concentrated to obtain crude intermediate **25**.

In a separate flask, a solution of lithium tetramethylpiperidide was prepared by the dropwise addition of *n*-BuLi (14.0 mL, 22.4 mmol; 1.6 M solution in hexanes) to a solution of 2,2,6,6-tetramethylpiperidide (4.17 mL, 24.5 mmol) in THF (100 mL) at -78  $^\circ\text{C}$ . After a brief warm-up to rt, the solution was cooled to -78  $^\circ\text{C}$ , and crude intermediate **25** in THF (50 mL) was added dropwise over 30 min. After the addition, the reaction was stirred at -78  $^\circ\text{C}$  for 30 min and at -40  $^\circ\text{C}$  for another 30 min. The reaction was cooled again to -78  $^\circ\text{C}$  and quenched with acetic acid (3 mL). The reaction mixture was diluted in ether (100 mL), washed with water (3 x 100 mL), 0.5 N HCl (3 x 30 mL), and brine

(10 mL), dried ( $\text{MgSO}_4$ ), and concentrated. The crude product was purified by chromatography (ethyl acetate/hexanes, 3:17) to yield the major diastereomer (**26**) as a white solid (2.91 g, 36%).  $^1\text{H}$  NMR matched literature value.<sup>27</sup>  $^1\text{H}$  NMR (500 MHz,  $\text{CDCl}_3$ )  $\delta$  6.76 (d,  $J$  = 9.5 Hz, 1H), 4.22 (ddd,  $J$  = 9.6, 5.1, 1.8 Hz, 1H), 4.06 (s, 1H), 3.70 (s, 3H), 3.31 (s, 3H), 3.23 (dd,  $J$  = 10.9, 5.1 Hz, 1H), 2.80 (dd,  $J$  = 10.9, 1.9 Hz, 1H), 1.40 (s, 9H), 0.11 (s, 9H).  $^{13}\text{C}$  NMR (126 MHz,  $\text{CDCl}_3$ )  $\delta$  173.09, 155.37, 110.31, 79.39, 59.44, 52.83, 50.78, 49.65, 36.83, 28.50, 0.89. HRMS (LC-TOF): Calculated for  $\text{C}_{15}\text{H}_{29}\text{NO}_6\text{Si}$  [ $\text{M}+\text{Na}$ ]<sup>+</sup> 402.1377; found 402.1388.

**(S)-Methyl 4-((tert-butoxycarbonyl)amino)-4,5-dihydrothiophene-2-carboxylate (28)**

To a stirred solution of **26** (979 mg, 2.58 mmol) in 1 M HF solution (13 mL, prepared by diluting 48% aqueous HF in dry methanol) at rt was added TBAF (2.84 mL, 2.84 mmol; 1 M solution in THF). The reaction was stirred at rt for 2 h before being cooled in an ice/brine bath. Once cooled,  $\text{NaBH}_4$  (199 mg, 5.16 mmol) was added in small portions while maintaining a reaction temp of 0  $^\circ\text{C}$ . Following addition, the reaction was stirred for 1 h at 0  $^\circ\text{C}$  before being quenched with acetone (1.3 mL) and allowed to continue stirring at rt. After 1 h, acetic acid (161  $\mu\text{L}$ ) was added, followed by removal most of the solvent under reduced pressure. The resulting crude mixture was diluted with ethyl acetate (30 mL) and washed with 1:1 saturated brine:water (15 mL), water (2 x 15 mL), and brine (3 mL), dried ( $\text{MgSO}_4$ ), and concentrated to yield the crude alcohol, which was used in the next step without purification.

To a stirred solution of the crude alcohol in  $\text{CH}_2\text{Cl}_2$  (13 mL) at 0  $^\circ\text{C}$  was added  $\text{Et}_3\text{N}$  (1.44 mL, 10.3 mmol), followed by mesyl chloride (400  $\mu\text{L}$ , 5.17 mmol) dropwise. The reaction was stirred for 30 min at 0  $^\circ\text{C}$  and overnight at rt. After removal of most of the solvent under reduced pressure, the resulting crude mixture was diluted with ethyl ether (30 mL), washed with water (2x 15 mL), 0.5 M HCl (15 mL), and brine (3 mL), dried ( $\text{MgSO}_4$ ), and concentrated. Chromatography (ethyl acetate/hexanes, 3:7) afforded the desired product as a white solid (430 mg, 64%).  $^1\text{H}$  NMR (500 MHz,  $\text{CDCl}_3$ )  $\delta$  6.51 (d,  $J$  = 3.3 Hz, 1H), 5.15 (m, 1H), 4.90 (d,  $J$  = 9.2 Hz, 1H), 3.79 (s, 3H), 3.61 (dd,  $J$  = 12.3, 8.3 Hz, 1H), 3.13 (dd,  $J$  = 12.3, 4.2 Hz, 1H), 1.43 (s, 9H).  $^{13}\text{C}$  NMR (126 MHz,  $\text{CDCl}_3$ )  $\delta$  162.68, 154.74, 138.37, 131.93, 80.35, 58.29, 52.76, 39.40, 28.44. HRMS (LC-TOF): Calculated for  $\text{C}_{11}\text{H}_{17}\text{NO}_4\text{S}$  [ $\text{M}+\text{Na}$ ]<sup>+</sup> 282.0770; found 282.0773.

**(2S,4S)- and (2R,4S)-Methyl 4-((tert-butoxycarbonyl)amino)tetrahydrothiophene-2-carboxylate (29 and 30):**

Magnesium turnings (484 mg, 19.9 mmol) were added to a mixture of (*S*)-methyl 4-((tert-butoxycarbonyl)amino)-4,5-dihydrothiophene-2-carboxylate (**28**, 430 mg, 1.66 mmol) and  $\text{NH}_4\text{Cl}$  (5.33 g, 99.6 mmol) in MeOH (15 mL), and the resulting mixture was vigorously stirred overnight at rt. After removal of most of the solvent under reduced pressure, the resulting crude mixture was diluted with water (20 mL) and extracted with ethyl ether (3 x 40 mL). The combined organics were washed with brine (2 mL),

dried (MgSO<sub>4</sub>), and concentrated. Chromatography (ethyl ether/toluene, 2:8) afforded **29** (109 mg, 25%) and **30** (141 mg, 32%) as white solids. (**29**): <sup>1</sup>H NMR (500 MHz, CDCl<sub>3</sub>) δ 5.86 (d, *J* = 7.6 Hz, 1H), 4.55-4.40 (m, 1H), 3.97 (dd, *J* = 8.6, 3.1 Hz, 1H), 3.72 (s, 3H), 3.11 (dd, *J* = 11.0, 5.0 Hz, 1H), 2.92 (dd, *J* = 11.3, 3.6 Hz, 1H), 2.37-2.26 (m, 1H), 2.17 (ddd, *J* = 14.0, 8.5, 6.0 Hz, 1H), 1.41 (s, 9H); <sup>13</sup>C NMR (126 MHz, CDCl<sub>3</sub>) δ 175.10, 155.31, 79.48, 55.54, 52.95, 45.68, 40.16, 37.28, 28.48; HRMS (LC-TOF): Calculated for C<sub>11</sub>H<sub>19</sub>NO<sub>4</sub>S [M+Na]<sup>+</sup> 284.0927, found 284.0931. (**30**): <sup>1</sup>H NMR (500 MHz, (CD<sub>3</sub>)<sub>2</sub>CO) δ 6.25 (d, *J* = 3.4 Hz, 1H), 4.49 (tt, *J* = 7.4, 3.8 Hz, 1H), 4.06 (dd, *J* = 7.5, 5.1 Hz, 1H), 3.69 (s, 3H), 3.14 (dd, *J* = 10.5, 5.6 Hz, 1H), 2.78 (dd, *J* = 10.5, 6.2 Hz, 1H), 2.42 (dt, *J* = 13.0, 5.3 Hz, 1H), 2.15-2.05 (m, 1H), 1.42 (s, 9H); <sup>13</sup>C NMR (126 MHz, (CD<sub>3</sub>)<sub>2</sub>CO) δ 174.00, 155.92, 78.96, 55.98, 52.52, 44.49, 37.69, 37.53, 28.53; HRMS (LC-TOF): Calculated for C<sub>11</sub>H<sub>19</sub>NO<sub>4</sub>S [M+Na]<sup>+</sup> 284.0927, found 284.0931.

**(2*S*,4*S*)-4-Aminotetrahydrothiophene-2-carboxylic acid hydrochloride (**17**):**

Boc-protected amino acid ester **29** (100 mg, 0.38 mmol) was dissolved in 4 N HCl (5 mL) and acetic acid (5 mL). The resulting solution was heated to 70 °C and stirred for 5 h before being concentrated in vacuo to afford a solid. The solid was purified by ion-exchange chromatography (AG 50W-X8), eluting with a gradient from 0.4 N to 2.0 N HCl, giving the desired amino acid hydrochloride product as a white solid (63 mg, 89%). <sup>1</sup>H NMR (500 MHz, MeOD) δ 4.10 (m, 2H), 3.32 (dd, *J* = 11.8, 5.6 Hz, 1H), 3.09 (dd, *J* = 11.8, 5.0 Hz, 1H), 2.52 - 2.43 (m, 1H). <sup>13</sup>C NMR (126 MHz, MeOD) δ 177.11, 55.99, 46.14, 37.28, 36.77. HRMS (LC-TOF): Calculated for C<sub>5</sub>H<sub>9</sub>NO<sub>2</sub>S [M-H]<sup>-</sup> 146.0281; found 146.0278.

**(2*R*,4*S*)-4-Aminotetrahydrothiophene-2-carboxylic acid hydrochloride (**18**):**

Compound **18** (61 mg, 87%) was synthesized from **30** (100 mg, 0.38 mmol) using a similar procedure to that for **17** from **29**. <sup>1</sup>H NMR (500 MHz, MeOD) δ 4.15 (p, *J* = 5.9 Hz, 1H), 4.05 (dd, *J* = 7.6, 4.5 Hz, 1H), 3.28 (dd, *J* = 11.6, 5.7 Hz, 1H), 2.95 (dd, *J* = 11.5, 5.7 Hz, 1H), 2.65 (dt, *J* = 13.6, 5.0 Hz, 1H), 2.18 (dt, *J* = 13.9, 7.2 Hz, 1H). <sup>13</sup>C NMR (126 MHz, MeOD) δ 175.62, 55.75, 45.19, 37.22, 35.81. HRMS (LC-TOF): Calculated for C<sub>5</sub>H<sub>9</sub>NO<sub>2</sub>S [M-H]<sup>-</sup> 146.0281; found 146.0278.

**(4*S*)-Methyl 4-((*tert*-butoxycarbonyl)amino)tetrahydrothiophene-2-carboxylate 1,1-dioxide (**31**):**

To a stirred solution of **29** (60 mg, 0.23 mmol) and MnSO<sub>4</sub>·H<sub>2</sub>O (1 mg) in CH<sub>3</sub>CN (5 mL) was added at room temperature a mixture of 30% H<sub>2</sub>O<sub>2</sub> (1.15 mmol, 118 μL) and 0.2 M NaHCO<sub>3</sub> (3.4 mL), previously prepared at 0 °C. After 15 min the reaction was quenched with brine, extracted with ethyl acetate (3 x 10 mL), dried (Na<sub>2</sub>SO<sub>4</sub>), and concentrated. Chromatography (ethyl acetate/hexanes; 1:9) provided the desired product as a 1:1 mixture of the two diastereomers (55 mg, 81%). <sup>1</sup>H NMR (500 MHz, CDCl<sub>3</sub>) δ [5.57 (d, *J* = 7.1 Hz); 5.21 (d, *J* = 6.2 Hz), 1H], [4.65 (br s), 4.54 (sex, *J* = 6.6 Hz), 1H], [4.14 (t, *J* = 7.9 Hz), 4.11

(dd, *J* = 9.1, 6.1 Hz), 1H], [3.88 (s), 3.85 (s), 3H], [3.47 (dd, *J* = 13.5, 6.9 Hz), 3.42 (dd, *J* = 13.7, 7.0 Hz), 1H], [3.18 (t, *J* = 4.9 Hz), 3.15 (t, *J* = 5.4 Hz), 1H], [2.83 (dt, *J* = 13.9, 6.8 Hz), 2.69 (ddd, *J* = 14.1, 8.9, 6.9 Hz), 1H], 2.50 (m, 1H), 1.44 (s, 9H). <sup>13</sup>C NMR (126 MHz, CDCl<sub>3</sub>) δ [166.49, 165.77], [155.00, 154.78], [80.76, 80.59], [65.14, 64.02], [57.07, 56.05], [53.98, 53.78], [45.54, 45.37], [33.30, 32.23], [28.43, 28.41]. HRMS (LC-TOF): Calculated for C<sub>11</sub>H<sub>19</sub>NO<sub>6</sub>S [M+Na]<sup>+</sup> 316.0825; found 316.0833.

**(4*S*)-4-Aminotetrahydrothiophene-2-carboxylic acid 1,1-dioxide hydrochloride (**19**):**

Compound **19** was synthesized from **31** as an inseparable 1:1 mixture of diastereomers using a procedure similar to that for **17** from **29** (86%). <sup>1</sup>H NMR (500 MHz, MeOD) δ [4.41 (dd, *J* = 8.6, 4.9 Hz), 4.36 (dd, *J* = 9.5, 7.9 Hz), 1H], [4.27 (p, *J* = 7.4 Hz), 4.12 (p, *J* = 8.1 Hz), 1H], [3.73 (dd, *J* = 13.8, 8.1 Hz), 3.68 (dd, *J* = 13.8, 8.0 Hz), 1H], [3.35 (dd, *J* = 13.9, 7.1 Hz), 3.29 (dd, *J* = 13.5, 8.1 Hz), 1H], [2.96 (ddd, *J* = 14.2, 7.0, 5.0 Hz), 2.84 (dt, *J* = 14.2, 7.2 Hz), 1H], [2.55 (dt, *J* = 13.9, 9.3 Hz), 2.46 (dt, *J* = 14.3, 8.1 Hz), 1H]. <sup>13</sup>C NMR (126 MHz, MeOD) δ [167.13, 167.04], [66.52, 65.56], [54.61, 54.44], [46.38, 45.40], [31.40, 31.37]. HRMS (LC-TOF): Calculated for C<sub>5</sub>H<sub>9</sub>NO<sub>4</sub>S [M+Na]<sup>+</sup> 202.0144; found 202.014.

**(1*R*,4*S*)-2-azabicyclo[2.2.1]heptan-3-one (**38**):**

Compound **38** was prepared from (1*S*,4*R*)-2-azabicyclo[2.2.1]hept-5-en-3-one (**37**) by following a published procedure (94%).<sup>36</sup> <sup>1</sup>H NMR matched literature value.<sup>37</sup> <sup>1</sup>H NMR (500 MHz, CDCl<sub>3</sub>) δ 5.53 (br s, 1H), 3.90 (m, 1H), 2.76 (m, 1H), 1.95-1.40 (m, 6H). <sup>13</sup>C NMR (126 MHz, CDCl<sub>3</sub>) δ 181.05, 55.54, 45.04, 41.37, 30.34, 23.79. HRMS (LC-TOF): Calculated for C<sub>6</sub>H<sub>9</sub>NO [M+Na]<sup>+</sup> 134.0576; found 134.0578.

**Preparation of (1*S*,3*R*)-3-aminocyclopentane-1-carboxylic acid (**39**):**

Compound **39** was prepared from **38** by following a published procedure (80%).<sup>37</sup> <sup>1</sup>H NMR matched literature value.<sup>37</sup> <sup>1</sup>H NMR (500 MHz, D<sub>2</sub>O) δ 3.76 (m, 1H), 3.01 (m, 1H), 2.44-1.79 (m, 6H). <sup>13</sup>C NMR (126 MHz, D<sub>2</sub>O) δ 180.01, 51.47, 42.40, 33.65, 29.81, 27.68. HRMS (LC-TOF): Calculated for C<sub>6</sub>H<sub>11</sub>NO<sub>2</sub> [M+H]<sup>+</sup> 130.0863; found 130.0864.

**Purification of GABA Aminotransferase (GABA-AT) from Pig Brain**

GABA-AT was isolated and purified from pig brain by a published procedure.<sup>38</sup> The purified GABA-AT used in these experiments was found to have a concentration of 6.41 mg/mL with a specific activity of 1.84 units/mg.

**Evaluation of Compounds as Time-Dependent Inhibitors of GABA-AT**

GABA-AT (17.5 μL) was incubated in the presence of varying concentrations of each compound (70 μL final volume) at 25 °C in 50 mM potassium pyrophosphate buffer solution, pH 6.5, containing 5 mM α-ketoglutarate and 1 mM β-mercaptoethanol. Aliquots (10 μL) were withdrawn at timed intervals and were added immediately to the assay solution (137 μL, see below) followed by the addition of SSDH (3 μL). The relative enzyme activity was determined by normalizing the rate of increasing absorbance

at 340 nm to a control. A Kitz and Wilson replot was used to determine the kinetic constants  $K_1$  and  $k_{\text{inact}}$ .<sup>29</sup>

### Evaluation of Compounds as Inhibitors of GABA-AT

Inhibition constants were determined by monitoring GABA-AT activity in the presence of 0–50 mM concentrations of synthesized analogues using a coupled assay with the enzyme succinic semialdehyde dehydrogenase (SSDH). The assay solution consisted of 10 mM GABA, 5 mM  $\alpha$ -ketoglutarate, 1 mM  $\text{NADP}^+$ , 5 mM  $\beta$ -mercaptoethanol, and excess SSDH in 50 mM potassium pyrophosphate buffer, pH 8.5. Enzyme activity was determined by observing the change in absorbance at 340 nm at 25 °C.  $\text{IC}_{50}$  values were obtained using non-linear regression in GraphPad Prism5 software. Subsequent  $K_i$  values were determined using the Cheng-Prusoff relationship.<sup>39</sup>

### Evaluation of Compounds as Substrates for GABA-AT

Compounds were tested using an experiment in which the conversion of  $\alpha$ -ketoglutarate to *L*-glutamic acid was monitored as an indication of the rate of PLP reduction to PMP, which in turn corresponds to amine oxidation to the corresponding aldehyde. Enzyme reactions were prepared at 5 mM concentrations of compounds in 100  $\mu\text{L}$  pyrophosphate buffer (50 mM, pH 8.5) containing 5 mM  $\alpha$ -ketoglutarate and 0.13 mg/mL purified GABA-AT and allowed to incubate at room temperature for 24 h. The *L*-glutamic acid content was determined by combining 50  $\mu\text{L}$  of each incubation mixture with 50  $\mu\text{L}$  of Tris-HCl buffer (100 mM, pH 7.5) containing 100  $\mu\text{M}$  Ampliflu™ Red (Sigma-Aldrich), 0.25 units/mL horseradish peroxidase and 0.08 units/mL *L*-glutamate oxidase in a 96-well black walled plate. After incubation at 37 °C for 30 min fluorescence was recorded with the aid of a microplate reader (BioTek Synergy H1) with 530 nm excitation and 590 nm emission wavelengths, where fluorescence is proportional to the *L*-glutamate concentration.

### Preparation of [7-<sup>3</sup>H]-Pyridoxal 5'-Phosphate ([7-<sup>3</sup>H]PLP)

To a solution of pyridoxal 5'-phosphate (PLP) in water (1.8 mL, 0.28 M) was added thirty drops of 1 M NaOH. The mixture was then cooled to 0 °C in an ice bath, and a solution of  $\text{NaBH}_4$  (5.86 mg, 0.15 mmol) and  $\text{NaB}^{[3}\text{H}]_4$  (100 mCi) in 450  $\mu\text{L}$  of 0.1 M NaOH was added in small portions and stirred for 1 h at 0 °C. Concentrated HCl (120  $\mu\text{L}$ ) was then added to the solution very slowly (the pH of the resulting solution was 4), and the reaction was stirred for 5 min at 0 °C. Ground  $\text{MnO}_2$  (200 mg, 2.3 mmol) was added, and the resulting mixture was stirred for 2 h at rt. A solution of 1 M NaOH was added dropwise to bring the pH to 8, and the resulting solution was centrifuged. The supernatants were collected and loaded onto a gel filtration column packed with Bio-Rad AG1-X8 resin (hydroxide form). Water and 5 M acetic acid was used as the mobile phase (gradient from 90% water to 0% water, 1.5 mL/min, 300 min). Fractions (10 mL each) were collected and tested for UV absorption and radioactivity. The fractions with the desired product were lyophilized and then loaded onto an HPLC with a Phenomenex Gemini C18

column (4.6 mm  $\times$  250 mm, 5  $\mu$ , 110 Å). Water (with 0.1% TFA) and acetonitrile (with 0.1% TFA) were used as the mobile phase (5% acetonitrile, 0.5 mL/min, 25 min; then gradient to 95% acetonitrile, 0.5 mL/min, 20 min). Under these conditions, PLP eluted at 38 min. Fractions running with the PLP peak were collected, counted for radioactivity using liquid scintillation counting, and then lyophilized, affording [7-<sup>3</sup>H]PLP.

### Preparation of [7-<sup>3</sup>H]PLP-Reconstituted GABA-AT

To potassium phosphate buffer (0.5 mL, 100 mM, pH 7.4) containing  $\beta$ -mercaptoethanol (0.25 mM) (buffer A) and GABA-AT (170  $\mu\text{g}$ , 1.55 nmol) protected from light was added GABA (10 mg, 0.097 mmol). The resulting solution was stirred at rt for 1 h and then was dialyzed at 4 °C against potassium phosphate buffer (200 mL, 500 mM, pH 5.5) containing  $\beta$ -mercaptoethanol (0.25 mM) (buffer B) and GABA (4.0 g, 39 mmol) for 3 h. The solution was then dialyzed at 4 °C against 1800 mL of buffer B overnight, followed by dialysis at 4 °C against 4  $\times$  500 mL of potassium phosphate buffer (100 mM, pH 8.0) containing  $\beta$ -mercaptoethanol (0.25 mM) (buffer C) at 1.5 h interval. An aliquot (1  $\mu\text{L}$ ) of the dialyzed solution was assayed to confirm that there was no enzyme activity remaining. To the dialyzed solution of enzyme (apo-GABA-AT) was added a solution of PLP (40  $\mu\text{L}$ , 20 mM) and [<sup>3</sup>H]PLP (1/5 the amount prepared above) and stirred at rt for 5 h until the enzyme activity returned and the reactivation was complete. The excess [<sup>3</sup>H]PLP was removed from the reconstituted GABA-AT solution by centrifugation with 5  $\times$  400  $\mu\text{L}$  of buffer C using a 10K molecular weight cutoff filter. The resulting enzyme solution was dialyzed at 4 °C against 2 L of buffer A overnight, affording the [<sup>3</sup>H]PLP-reconstituted GABA-AT solution.

### Inactivation of [7-<sup>3</sup>H]PLP-Reconstituted GABA-AT by **17** and Cofactor Analysis

A 60  $\mu\text{L}$  portion of buffer A containing [7-<sup>3</sup>H]PLP-reconstituted GABA-AT (1/5 the amount prepared above),  $\alpha$ -ketoglutarate (3 mM), and **17** (4 mM) was protected from light and incubated at rt overnight until the activity of GABA-AT was less than 1%. To the inactivated enzyme solution was added KOH (1 drop, 1 M) to adjust the pH to 11. The mixture was allowed to stand at rt for 1 h, then trifluoroacetic acid (TFA) (6.7  $\mu\text{L}$ ) was added, and it was allowed to stand for another 5 min. The resulting denatured enzyme solution was centrifuged at 13,400 rpm for 5 min. The supernatant was collected, and the pellet was rinsed with 2  $\times$  50  $\mu\text{L}$  of buffer A containing 10% TFA and centrifuged. The supernatant and rinses were combined and lyophilized. The resulting solid was dissolved in 100  $\mu\text{L}$  of a solution containing 1 mM PLP and 1 mM PMP standards and injected into an HPLC with an Econosil C18 column (4.6 mm  $\times$  150 mm, 10  $\mu$ ). Water (with 0.1% TFA) and acetonitrile (with 0.1% TFA) were used as the mobile phase (0% acetonitrile, 0.5 mL/min, 25 min; then gradient to 90% acetonitrile, 1.0 mL/min, 30 min). Under these conditions, PMP eluted at 8 min and PLP at 13 min. Fractions were collected every minute, and the radioactivity was measured by liquid scintillation counting.

### Mass spectrometric analysis of the Inactivated GABA-AT

A 50  $\mu\text{L}$  portion of ammonium bicarbonate buffer (50 mM, pH 7.4) containing GABA-AT (23  $\mu\text{g}$ , 0.21 nmol),  $\alpha$ -ketoglutarate (5 mM), and **17** (43 mM) was protected from light and incubated at rt overnight until the activity of GABA-AT was less than 1%. Another 50  $\mu\text{L}$  of ammonium bicarbonate buffer (50 mM, pH 7.4) containing GABA-AT (23  $\mu\text{g}$ , 0.21 nmol) and  $\alpha$ -ketoglutarate (5 mM) was subjected to the same condition as a control. After incubation, formic acid (10  $\mu\text{L}$ ) was added to each sample, and 20  $\mu\text{L}$  of each resulting solution was loaded onto a 5- $\mu\text{m}$  Luna C18 column (2 mm i.d.; 150 mm) (Phenomenex, Torrance, CA, USA). A 30-min LC gradient was employed at a flow rate of 200  $\mu\text{L}/\text{min}$  on an Agilent 1150 LC system (Agilent, Santa Clara, CA, USA). Mass spectrometry was performed on a Q-Exactive mass spectrometer (Thermo Fisher Scientific, Waltham, MA, USA). Intact MS spectra were acquired at a resolution of 35,000. The top-five most intense ions were selected for fragmentation in a data-dependent acquisition mode. Mass spectra were acquired at a resolution of 17,500.

### Crystallization and Data Collection

Potassium pyrophosphate buffer (500  $\mu\text{L}$ , 50 mM, pH 8.5) containing GABA-AT (200  $\mu\text{g}$ , 1.82 nmol),  $\alpha$ -ketoglutarate (5 mM),  $\beta$ -mercaptoethanol (5 mM), and **17** (37 mM) was protected from light and incubated at rt overnight until the activity of GABA-AT was less than 3%. The inactivated GABA-AT was then buffer-exchanged into a sodium acetate buffer (40 mM, pH 5.5) by centrifugation before the initial crystallization screening and optimization. The crystals were obtained in hanging drops comprising 1  $\mu\text{L}$  of 10 mg/mL inactivated GABA-AT and 1  $\mu\text{L}$  reservoir solution, containing 0.1 M ammonium acetate, 0.1 M Bis-Tris (pH 5.5), and 17% w/v PEG 10,000. Diffraction quality crystals grew within 4-5 days at ambient temperature. For X-ray data collection, these crystals were briefly soaked in the reservoir solution with additional 20% (v/v) glycerol as cryo-protectant before flash freezing in liquid nitrogen. Crystallographic data were collected on beamlines 23ID-B and 23ID-D of GM/CA@APS of the Advanced Photon Source (APS) using X-rays of 0.99  $\text{\AA}$  wavelength and Rayonix (formerly MAR-USA) 4 $\times$ 4 tiled CCD detector with a 300 mm<sup>2</sup> sensitive area. All data were indexed, integrated, and scaled with HKL2000. Data collection and processing statistics are given in Table S1.

### Phasing, Model Building, and Refinement

Molecular replacement for the inactivated GABA-AT was carried out using the program Phaser from CCP4 software suite.<sup>40</sup> The tetrameric structure of native GABA-AT from pig brain was used as the starting search model, in which all solvent and PLP molecules were deleted. Initial  $R_{\text{free}}$  and R factor of the correct solution were 29.59% and 28.91%, respectively. The rigid body refinement was followed by restrained refinement with Refmac5<sup>41</sup> and further manual model inspection and adjustments with Coot.<sup>42</sup> When refinement converged, the Fo-Fc difference maps, before incorporation of ligands in the structures,

show a well-defined electron density for both PLP and the inactivator tetrahydrothiophene (Figure 4A). The structure of inactivator tetrahydrothiophene was built in Chemdraw (a "Mol" file); the molecule was regularized and then the chemical restraints were generated in program JLigand.<sup>43</sup> The PLP and the inactivator were fitted into the residual electron density in COOT after the rest of the structure, including most of the solvent molecules, had been refined. The  $R_{\text{free}}$  and  $R_{\text{factor}}$  for inactivated GABA-AT were 21.5% and 19.8%, respectively (Supporting Information Table S1). All structural figures were made in UCSF Chimera.<sup>44</sup>

## ASSOCIATED CONTENT

### Supporting Information

NMR spectroscopy, mass spectroscopy, and crystallographic data collection and processing statistics. This material is available free of charge via the Internet at <http://pubs.acs.org>.

## AUTHOR INFORMATION

### Corresponding Author

\* Agman@chem.northwestern.edu

## ACKNOWLEDGMENT

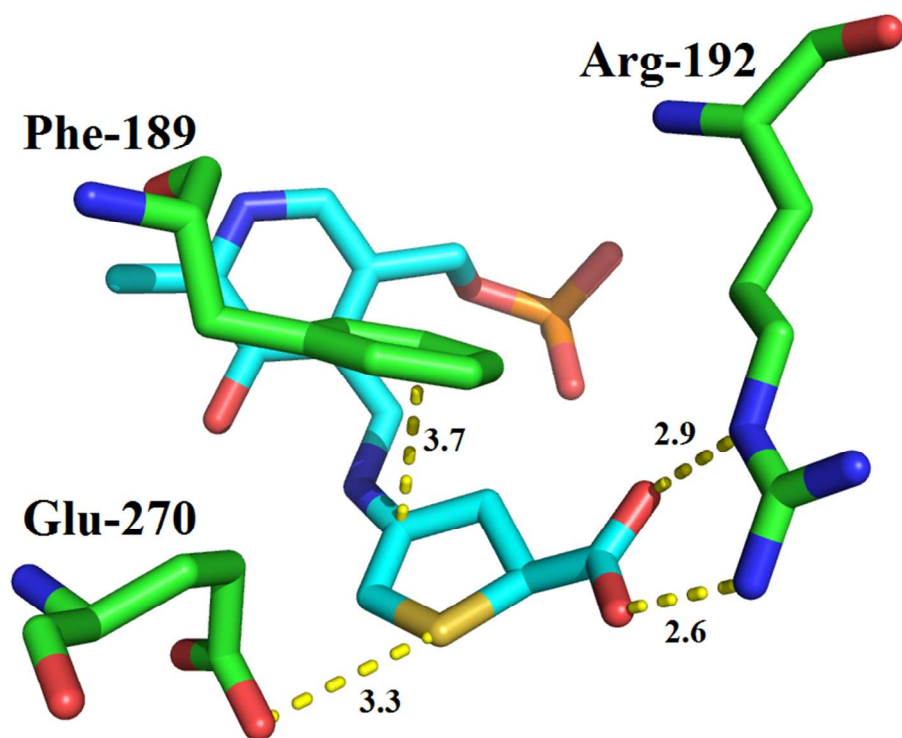
We are grateful to the National Institutes of Health for financial support (Grants GM066132 and DA030604 to RBS; GM067725 to NLK). GM/CA@APS has been funded in whole or in part with Federal funds from the National Cancer Institute (ACB-12002) and the National Institute of General Medical Sciences (AGM-12006). This research used resources of the Advanced Photon Source, a U.S. Department of Energy (DOE) Office of Science User Facility operated for the DOE Office of Science by Argonne National Laboratory under Contract No. DE-AC02-06CH11357. The authors wish to thank Drs. Jose Juncosa and Hyunbeom Lee for helpful discussions and Dr. Boobalan Pachaiyappan for constructing the computer model of **39** docked into the enzyme using GOLD (Supporting Information Figure S25). The authors would also like to thank Park Packing Co. (Chicago, IL) for their generosity in providing fresh pig brains for this study. Support for the spectrometer funding has been provided by the International Institute of Nanotechnology.

## REFERENCES

- (1) Chapter 1: Basic Mechanisms Underlying Seizures and Epilepsy. In *An Introduction to Epilepsy [Internet]*; Bromfield, E. B.; Cavazos, J. E.; Sirven, J. I., Eds.; American Epilepsy Society: West Hartford, CT, 2006.
- (2) Epilepsy Foundation. About Epilepsy: The Basics. <http://www.epilepsy.com/learn/about-epilepsy-basics> (accessed Jul 29, 2014).
- (3) Karlsson, A.; Fonnum, F.; Malthe-Sørensen, D.; Storm-Mathisen, J. *Biochem. Pharmacol.* **1974**, *23*, 3053-3061.
- (4) Baxter, C. F.; Roberts, E. *J. Biol. Chem.* **1958**, *233*, 1135-1139.
- (5) Durkin, M. M.; Smith, K. E.; Borden, L. A.; Weinshank, R. L.; Branchek, T. A.; Gustafson, E. L. *Mol. Brain. Res.* **1995**, *33*, 7-21.
- (6) Yogeeswari, P.; Sriram, D.; Vaigundaragavendran, J. *Curr. Drug Metab.* **2005**, *6*, 127-139.
- (7) Nishino, N.; Fujiwara, H.; Noguchi-Kuno, S. A.; Tanaka, C. *Jpn. J. Pharmacol.* **1988**, *48*, 331-339.

- (8) Aoyagi, T.; Wada, T.; Nagai, M.; Kojima, F.; Harada, S.; Takeuchi, T.; Takahashi, H.; Hirokawa, K.; Tsumita, T. *Chem. Pharm. Bull.* **1990**, *38*, 1748–1749.
- (9) Iversen, L. L.; Bird, E. D.; Mackay, A. V.; Rayner, C. N. *J. Psychiatr. Res.* **1974**, *11*, 255–256.
- (10) Dewey, S. L.; Morgan, A. E.; Ashby, C. R.; Horan, B.; Kushner, S. A.; Logan, J.; Volkow, N. D.; Fowler, J. S.; Gardner, E. L.; Brodie, J. D. *Synapse* **1998**, *30*, 119–129.
- (11) Gale, K. *Epilepsia* **1989**, *30 Suppl 3*, S1–11.
- (12) Van Gelder, N. M.; Elliott, K. A. C. *J. Neurochem.* **1958**, *3*, 139–143.
- (13) Singh, J.; Petter, R. C.; Baillie, T. A.; Whitty, A. *Nat. Rev. Drug Discovery* **2011**, *10*, 307–317.
- (14) Lippert, B.; Metcalf, B. W.; Jung, M. J.; Casara, P. *Eur. J. Biochem.* **1977**, *74*, 441–445.
- (15) Waterhouse, E. J.; Mims, K. N.; Gowda, S. N. *Neuropsychiatr Dis Treat.* **2009**, *5*, 505–515.
- (16) Tassinari, C. A.; Michelucci, R.; Ambrosetto, G.; Salvi, F. *Arch. Neurol.* **1987**, *44*, 907–910.
- (17) Browne, T. R.; Mattson, R. H.; Penry, J. K.; Smith, D. B.; Treiman, D. M.; Wilder, B. J.; Ben-Menachem, E.; Miketta, R. M.; Sherry, K. M.; Szabo, G. K. *Br. J. Clin. Pharmacol.* **1989**, *27 Suppl 1*, 95S–100S.
- (18) Sivenius, M. R.; Ylinen, A.; Murros, K.; Matilainen, R.; Riekinen, P. *Epilepsia* **1987**, *28*, 688–692.
- (19) Sander, J. W.; Hart, Y. M.; Trimble, M. R.; Shorvon, S. D. *J. Neurol. Neurosurg. Psychiatry.* **1991**, *54*, 435–439.
- (20) Wild, J. M.; Chiron, C.; Ahn, H.; Baulac, M.; Burszty, J.; Gandolfo, E.; Goldberg, I.; Goñi, F. J.; Mercier, F.; Nordmann, J.-P.; Safran, A. B.; Schiefer, U.; Puccia, E. *CNS Drugs* **2009**, *23*, 965–982.
- (21) Nanavati, S. M.; Silverman, R. B. *J. Am. Chem. Soc.* **1991**, *113*, 9341–9349.
- (22) Choi, S.; Storic, P.; Schirmer, T.; Silverman, R. B. *J. Am. Chem. Soc.* **2002**, *124*, 1620–1624.
- (23) Pan, Y.; Qiu, J.; Silverman, R. B. *J. Med. Chem.* **2003**, *46*, 5292–5293.
- (24) Okumura, H.; Omote, M.; Takeshita, S. *Arzneimittelforschung.* **1996**, *46*, 459–462.
- (25) Pan, Y.; Gerasimov, M. R.; Kvist, T.; Wellendorph, P.; Madsen, K. K.; Pera, E.; Lee, H.; Schousboe, A.; Chebib, M.; Bräuner-Osborne, H.; Craft, C. M.; Brodie, J. D.; Schiffer, W. K.; Dewey, S. L.; Miller, S. R.; Silverman, R. B. *J. Med. Chem.* **2012**, *55*, 357–366.
- (26) Silverman, R. B. *J. Med. Chem.* **2012**, *55*, 567–575.
- (27) Adams, J. L.; Chen, T. M.; Metcalf, B. W. *J. Org. Chem.* **1985**, *50*, 2730–2736.
- (28) Fu, M.; Nikolic, D.; Van Breemen, R. B.; Silverman, R. B. *J. Am. Chem. Soc.* **1999**, *121*, 7751–7759.
- (29) Kitz, R.; Wilson, I. B. *J. Biol. Chem.* **1962**, *237*, 3245–3249.
- (30) Liu, D.; Pozharski, E.; Lepore, B. W.; Fu, M.; Silverman, R. B.; Petsko, G. A.; Ringe, D. *Biochemistry* **2007**, *46*, 10517–10527.
- (31) Iwaoka, M.; Takemoto, S.; Okada, M.; Tomoda, S. *Chem. Lett.* **2001**, 132–133.
- (32) Nagao, Y.; Hirata, T.; Goto, S.; Sano, S.; Kakehi, A.; Iizuka, K.; Shiro, M. *J. Am. Chem. Soc.* **1998**, *120*, 3104–3110.
- (33) Ioannidis, S.; Lamb, M. L.; Almeida, L.; Guan, H.; Peng, B.; Beberntz, G.; Bell, K.; Alimzhanov, M.; Zinda, M. *Bioorg. Med. Chem. Lett.* **2010**, *20*, 1669–1673.
- (34) Iwaoka, M.; Takemoto, S.; Tomoda, S. *J. Am. Chem. Soc.* **2002**, *124*, 10613–10620.
- (35) Jones, G.; Willett, P.; Glen, R. C. *J. Mol. Biol.* **1995**, *245*, 43–53.
- (36) Evans, C.; McCague, R.; Roberts, S. M.; Sutherland, A. G. *J. Chem. Soc., Perkin Trans. 1* **1991**, 656–657.
- (37) Forró, E.; Fülöp, F. *Eur. J. Org. Chem.* **2008**, *2008*, 5263–5268.
- (38) Koo, Y. K.; Nandi, D.; Silverman, R. B. *Arch. Biochem. Biophys.* **2000**, *374*, 248–254.
- (39) Yung-Chi, C.; Prusoff, W. H. *Biochem. Pharmacol.* **1973**, *22*, 3099–3108.
- (40) Collaborative Computational Project Number 4 *Acta Crystallogr. D Biol. Crystallogr.* **1994**, *50*, 760–763.
- (41) Emsley, P.; Cowtan, K. *Acta Crystallogr. D Biol. Crystallogr.* **2004**, *60*, 2126–2132.
- (42) Murshudov, G. N.; Vagin, A. A.; Dodson, E. J. *Acta Crystallogr. D Biol. Crystallogr.* **1997**, *53*, 240–255.
- (43) Lebedev, A. A.; Young, P.; Isupov, M. N.; Moroz, O. V.; Vagin, A. A.; Murshudov, G. N. *Acta Crystallogr. D Biol. Crystallogr.* **2012**, *68*, 431–440.
- (44) Pettersen, E. F.; Goddard, T. D.; Huang, C. C.; Couch, G. S.; Greenblatt, D. M.; Meng, E. C.; Ferrin, T. E. *J. Comput. Chem.* **2004**, *25*, 1605–1612.

Insert Table of Contents artwork here

32  
33  
34  
35  
36  
37  
38  
39  
40  
41  
42  
43  
44  
45  
46  
47  
48  
49  
50  
51  
52  
53  
54  
55  
56  
57  
58  
59  
60